2021

Quasi Steady-State Modeling Approach for Low Computational Cost Design Optimization of Heat Exchangers for Phase Change Material (PCM) Thermal Batteries

Adam Rhoads
Optimized Thermal Systems, Inc.

Daniel Bacellar
Optimized Thermal Systems, Inc., dfbace@umd.edu

Cara Martin
Optimized Thermal Systems, Inc.

Remo Waser
Lucerne University of Applied Sciences and Arts, Switzerland

Maurizio Zaglio
Sunamp, Ltd., Scotland

See next page for additional authors

Authors

Adam Rhoads, Daniel Bacellar, Cara Martin, Remo Waser, Maurizio Zaglio, Hal Stillman, Jörg Worlitschek, and Simon Maranda

Quasi Steady-State Modeling Approach for Low Computational Cost Design Optimization of Heat Exchangers for Phase Change Material (PCM) Thermal Batteries

Adam RHOADS[1*], Daniel BACELLAR[1], Cara MARTIN[1], Remo WASER[2], Maurizio ZAGLIO[3], Hal STILLMAN[4], Jörg WORLITSCHEK[2], Simon MARANDA[2]

[1]Optimized Thermal Systems, Inc. Beltsville, MD
(email: rhoads@optimizedthermalsystems.com)

[2]Lucerne University of Applied Sciences and Arts. Zürich, Switzerland

[3]Sunamp, Ltd. Tranent, Scotland

[4]International Copper Association, Ltd.

*Corresponding Author

ABSTRACT

Energy storage devices are key components to enable stable, more efficient, and controllable energy flow in systems. Furthermore, they are facilitators for maximizing the use of renewable primary energy sources, which often do not meet immediate supply-demand needs. Thermal batteries can be configured as tube and flat fin heat exchangers using water as working fluid inside the tubes and surrounded by a Phase-Change Material (PCM) on the external surface. These components typically require transient high-order modeling physics to simulate their behavior that are generally computationally intensive. This paper presents a low computational cost tool for design optimization of the heat exchangers for these batteries during discharge, i.e., solidification of the PCM. The approach consists of evaluating the heat transfer rate for an average PCM mass fraction of 50% and assuming a quasi-steady-state condition. The PCM thermal resistance is predicted using metamodels derived from validated CFD simulations. Using experimental data, the solver prediction matched the heat transfer rate during phase change from 2.3% to 22.9% for the same battery at different water inlet temperatures. The proposed solver is more than four orders of magnitude faster than the full transient model for a single design. This allows for using optimization such as Multi-Objective Genetic Algorithms (MOGA) to explore novel designs in only a few minutes. Finally, the optimization study suggested that for a particular battery, there is a trade-off where one may save more than 22% in material cost for the same performance or increase more than 6% in thermal performance for the same cost. Two distinct points in a Pareto front were selected and evaluated with the full transient model; the results provided good evidence that the proposed solver is sufficiently robust in predicting battery thermal performance and degradation.

1. INTRODUCTION

Thermal energy storage (TES) is any technology that stores thermal energy in a medium to be used later. This technology is often used in heating and cooling of buildings. Using thermal storage during peak hours of the day can save on energy costs by reducing the operation of traditional equipment. The thermal storage is then re-charged during off-peak hours when the cost of electricity is lower. Thermal storage devices can also lead to a higher penetration of renewables in thermal energy systems. Phase change materials (PCM) are often used as the medium for storing thermal energy. Tube-fin heat exchangers are often used to transfer heat from a fluid to the PCM in a thermal battery.

There have been many simulation tools for the modeling of thermal battery heat exchangers. The changing thermal resistance of the PCM needs to be modeled together with the thermal performance of the tube-fin heat exchanger. Neumann (2017) coupled a 1D heat exchanger model with a reduced 3D model of the PCM to capture the effect of phase change on the heat exchanger performance. In 2018, a new modeling method was presented by Waser et. al. (2018) at Lucerne University of Applied Science and Arts (HSLU). The HSLU model was split into two parts: a 3-dimensional model of the PCM surrounding the heat exchanger, and a 1-dimensional model of the heat exchanger that describes the fluid flow through the tubes. The results of the transient 3D model are used in a segment one-dimensional solver. The HSLU CFD model captures the PCM physics over time and has good absolute accuracy. While this modeling tool is detailed and accurate, it is computationally intensive, requiring hours to produce results for a single model. Such a tool provides a holistic performance assessment and can be used as a verification and validation tool but is challenging for use when more rapid comparative design evaluation is needed.

This paper describes a heat exchanger modeling tool developed to evaluate designs that provide higher capacity for lower material cost, at a low computation cost to allow for rapid design iteration. The new approach described herein evaluates heat exchanger designs at a single static operating condition representative of halfway of the solidification process, approximated as quasi steady-state condition. Such assumptions avoid the transient evaluation and provide a cost-effective optimization tool for relative performance changes. The heat exchanger model provides consistent trends and does not seek to provide precise absolute values. The HSLU CFD model was used as a validation tool to confirm the accuracy of the reduced modeling tool presented here.

2. MATERIALS & METHODS

2.1 Modeling Framework

2.1.1 Existing Transient Thermal Battery Model

The full transient model used to validate the steady-state tool presented here requires CFD simulations for every new heat exchanger design evaluation since it needs to predict the performance at every time-step. The model can handle both charging (melting) and discharging (solidification) of the thermal battery and captures the PCM physics over time with good absolute accuracy. It provides a holistic performance assessment and can be used as a reliable verification and validation tool. The model consists of a segmented one-dimensional fluid flow solver, coupled with CFD to evaluate the PCM side. Figure 1 shows the 3D CFD finite volume model of the PCM, and a diagram of the one-dimensional solver.

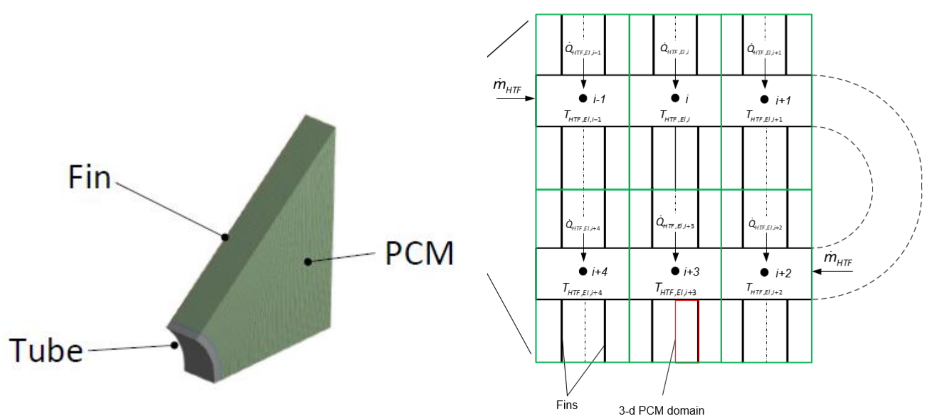

Figure 1: PCM transient model 3D model (Waser, Maranda, & Stamatious, 2018)

The CFD boundary conditions include constant convective heat transfer coefficient (HTC) and fluid temperature. The CFD domain consists of 1/8 of the PCM volume between the fins of a single tube, and the simulation outputs the heat load, temperature, and liquid mass fraction on a segment basis (Waser, Maranda, & Stamatious, 2018). This approach accurately models the PCM thermal resistance and allows the 1D model to evaluate the heat exchanger performance. This approach is suitable when evaluating individual thermal battery designs, but for rapid design evaluation this model structure would be time consuming.

2.1.2 New Heat Exchanger Model for Fast Evaluation

A new heat exchanger solver was developed to evaluate the performance of each design during thermal battery discharge. The new approach uses a quasi-steady state approach to model the tube-fin heat exchanger performance. and provide computationally efficient optimization tool for relative performance changes. The model breaks each heat exchanger tube into segments and solves them sequentially in the fluid flow direction. Figure 2 shows this tube discretization. The solver calculates outlet fluid temperature and total heat flow rate for an instantaneous condition, assumed to be representative of the solidification process.

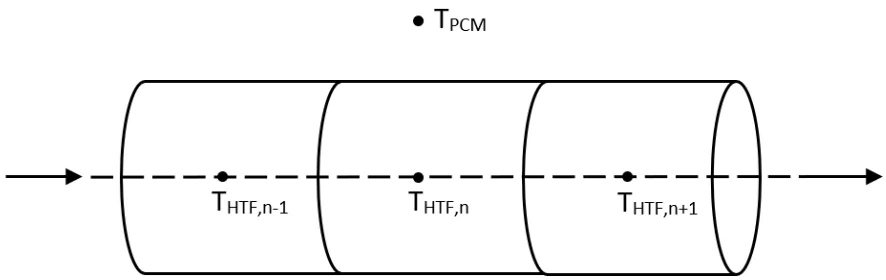

Figure 2: 1D heat exchanger tube solver

The heat transfer fluid pressure and enthalpy at the entry to each segment are used to determine the fluid temperature for that segment. The fluid state and the mass flow rate are used to determine the heat transfer coefficient (HTC) and pressure drop (DP). A single-phase HTC correlation (Gnielinski, 1976) and differential pressure correlation (Blasius, 1913) are used to calculate these values.

The fluid HTC and the thermal resistance due to PCM are used to calculate a total UA value for the segment. Equation 1 shows the calculation for the UA value of each heat exchanger segment.

$$UA_{seg} = \left(R_{PCM} + \frac{1}{UA_{HTF}}\right)^{-1} \tag{1}$$

The thermal resistance of PCM, R_{PCM}, is a function of the geometry of the heat exchanger, including the tube outer diameter, tube pitch, fin pitch, and fin thickness and is determined through approximation models, as described in the next section. Equation 2 shows this relationship. The segment UA value for the heat transfer fluid is determined by the convective HTC and the inside surface area of the tube. Equation 3 shows the convective heat transfer UA value calculation.

$$R_{PCM} = f(D_o, P_t, P_l, F_p, Thk_{fin}) \tag{2}$$

$$UA_{HTF} = \alpha_{HTF} * A_{seg} \tag{3}$$

This UA value is then used to calculate the heat load for the segment, and from that the outlet fluid enthalpy for the segment. Equation 4 shows the heat load calculation. From this the outlet fluid enthalpy is calculated. Equation 5 shows the outlet fluid enthalpy. The one-dimensional coil solver calls the segment solver in series along the fluid flow path until the end of coil is reached. The outlet state and overall heat transfer and pressure drop are then reported.

$$Q_{seg} = UA_{seg} * (T_{PCM} - T_{HTF}) \tag{4}$$

$$h_{HTF_{out}} = h_{HTF_{in}} * Q_{seg}/mdot \tag{5}$$

2.1.3 PCM Thermal Resistance

The heat exchanger solver determines the PCM thermal resistance using a metamodel derived from the transient CFD PCM model. The CFD model accurately predicts the thermal resistance during the discharge of PCM thermal energy, or the solidification of PCM from liquid state, based on the heat exchanger geometry. Figure 3 shows a schematic of the portion of the heat exchanger that was modeled.

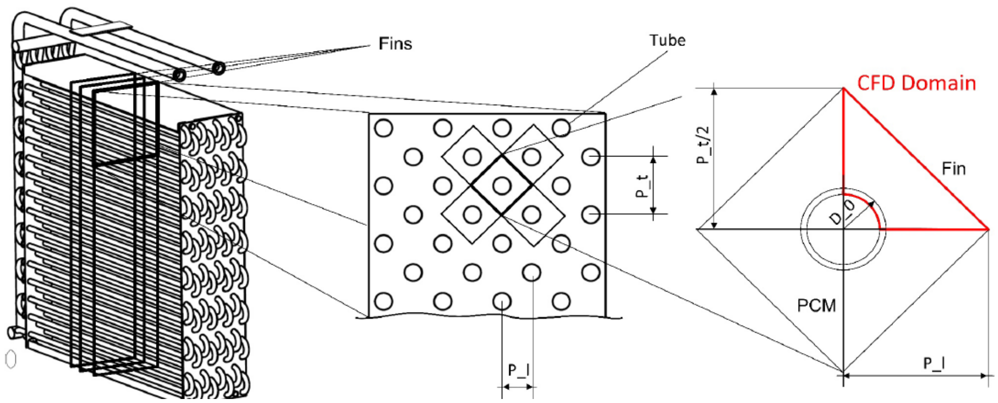

Figure 3: Schematic of CFD domain

DACE (2002), an open-source MATLAB toolbox, was used to generate the metamodel from simulation data. The thermal resistance metamodel lumps together the thermal resistance of the PCM and the thermal resistance of the heat exchanger tube and fin material. The metamodel predicts thermal resistance of the PCM and fin and tube material based on the heat exchanger geometry (outer tube diameter, tube pitch, fin density, fin thickness). Latin Hypercube Space Sampling (LHS) was used to develop a set of design of experiments to develop and test the metamodel. Table 1 shows the ranges of the variables varied in the LHS.

Table 1: Metamodel Latin Hypercube Space Sampling

Variable	Type	Lower Bound	Upper Bound
Outer diameter (OD) [mm]	Continuous	5	20
Vertical tube pitch ratio (Pt / OD)	Continuous	1.5	5
Horizontal tube pitch ratio (Pl / OD)	Continuous	1.5	5
Fin Pitch (FPI) [1/in]	Continuous	6	24
Fin Thickness (t) [mm]	Continuous	0.1	0.25

The PCM thermal resistance metamodels were validated against the full CFD model prediction. Model verification was conducted to compare the model prediction with unit test data. 250 validation points were evaluated using the CFD model. Metamodel verification was conducted against 25 of the designs. Figure 4 shows the comparison of the metamodel prediction against the simulation results of the more detailed model. Data from 250 simulation runs were reduced into a summary table of all design parameter combinations. The first 225 design evaluations were used to develop a metamodel for thermal resistance as a function of heat exchanger geometry.

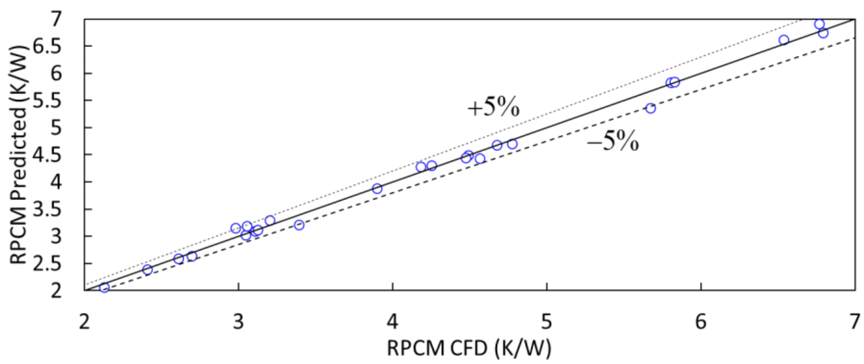

Figure 4: PCM thermal resistance metamodel versus CFD model prediction

The resulting R_{PCM} prediction was matched with 2.2% of more detailed simulation model. It was found that the average temperature was 2°C below saturation at 50% liquid fraction. Thermal resistance of the PCM at 50% liquid fraction is within 1% of the average across the phase-change region. This metamodel allows the heat exchanger solver to predict the PCM thermal resistance within 5% at many orders of magnitude faster than the CFD simulations.

2.1.4 PCM Phase Change Assumption

Thermal resistance of PCM in a thermal battery is a function of heat exchanger geometry, fluid temperature, and PCM mass fraction. To evaluate the heat exchanger at a quasi-steady-state condition and ignore the transient effect of PCM phase change, an assumption for average PCM mass fraction was made. For each heat exchanger geometry there exists a PCM mass fraction range where the average PCM temperature is roughly equal to the PCM phase change temperature, independent of fluid temperature; this generally falls in the 30-70% liquid fraction range. At mass fraction of 50%, the thermal resistance of the PCM is less sensitive to fluid temperature changes in properties and changes in thermal characteristics are negligible. From this review, it was assumed that the quasi steady-state model may neglect the mass fraction effect and assume that during phase change the thermal performance of the PCM is similar to the 50% mass fraction performance. The metamodel used to predict PCM thermal resistance uses a fixed mass fraction of 0.5 and only changes as a function of heat exchanger geometry.

3. RESULTS

3.1 Model Approach Verification

A verification was conducted of the heat exchanger solver against test data of a real thermal battery. Validation points were chosen from a transient test during the phase change of the battery. The selected points correspond to a region near the midpoint of the section where the water outlet temperature profile has the smallest slope, which is assumed to be the phase-change process. The heat load and water temperature profiles exhibited minimum slope near this time stamp, indicating that PCM phase change was occurring. Figure 5 shows a comparison of the test data to the model prediction.

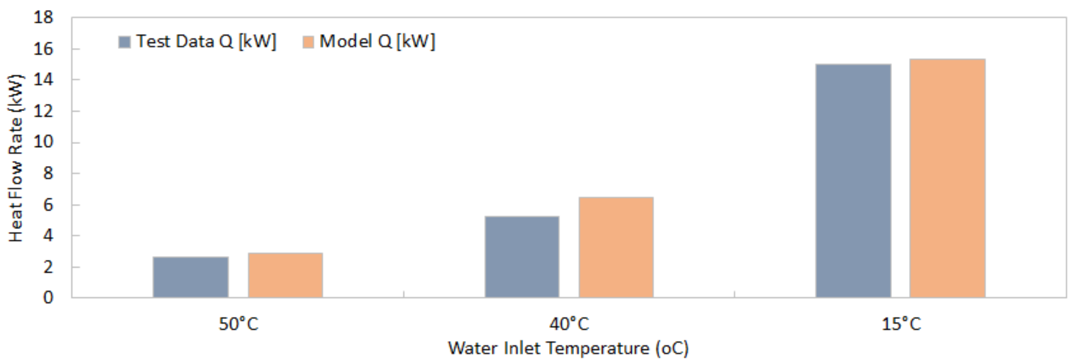

Figure 5: Model verification against experimental data

It was found that the model could predict heat capacity within 10% for the 50°C case, 2.3% for the 15°C case, and 22.9% for the 40°C case. In the latter case, the higher deviation can be largely attributed to the fact that a single time stamp from the test data was used instead of an averaging of multiple time stamp data points. Additionally, the model herein proposed aims to capture the trend as opposed to accuracy of the outputs.

3.2 Solver Verification and Validation

In addition to verification of the model performance of the baseline against test data, a study was conducted comparing solver performance to the transient CFD model. An initial heat exchanger optimization study was conducted, and two designs were selected to be validated. The solver heat load prediction of the designs was compared against the transient CFD model prediction. Table 2 shows the geometry parameters of the evaluated designs.

Table 2: Geometry parameters of verification designs

	D_o [mm]	P_t [mm]	P_l [mm]	FPI	thk_{fin} [mm]	Circuits	Rows
Baseline	7.0	25.4	12.5	9.6	0.1	8	16
Design A	5.7	21.3	20.5	9.9	0.1	5	19
Design B	5.6	13.4	16.9	10.6	0.1	6	30

The heat exchanger designs were modeled and simulated using the transient CFD model with an inlet water temperature of 15°C. Figure 6 displays the average PCM temperature and heat transfer rate of the PCM to the fluid over time for each of the three designs. During phase change the PCM average temperature stays roughly the same. It is in this region that the new model attempts to predict. To validate the performance prediction of the new model, a region of phase change was determined (between 190 and 230 seconds) and the heat transfer rate across this region was averaged. This value was compared against the new model prediction.

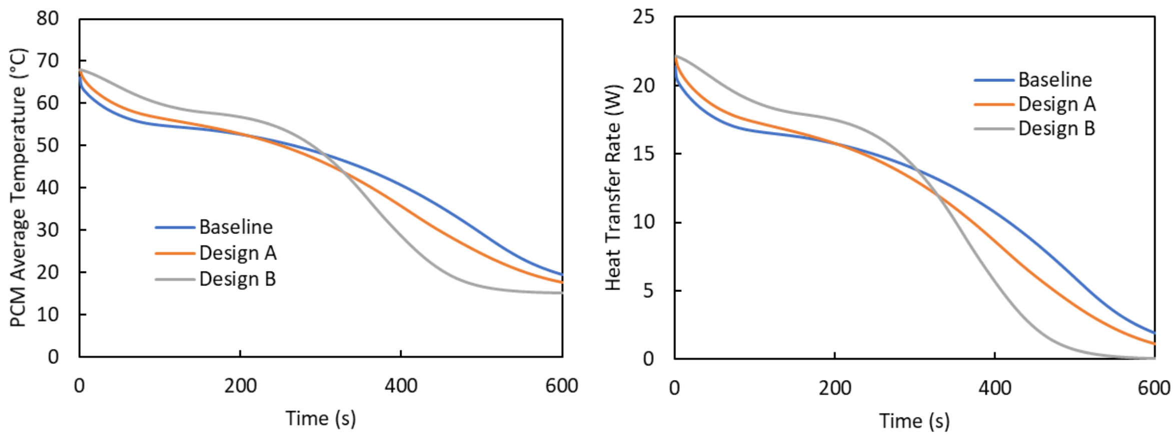

Figure 6: Transient CFD model heat PCM average temperature and heat transfer rate for selected designs

Table 3 displays a comparison of the CFD model phase change heat transfer prediction against the new solver heat transfer prediction. The solver predicts the performance of all three heat exchanger designs within 5%.

Table 3: Heat transfer prediction comparison

Design	CFD Model, Avg Q Across Phase Change [kW]	New Solver Model Q [kW]	% Deviation
Baseline	15.7	15.0	5%
Design A	15.7	15.4	2%
Design B	17.4	17.5	-1%

3.3 Optimization Study

An optimization study was conducted for a baseline thermal battery heat exchanger. The baseline design uses 7-mm outer diameter copper tubing with aluminum fins. Table 4 shows details of the baseline heat exchanger design.

Table 4: Baseline thermal battery details

	D_o [mm]	P_t Ratio [-]	P_l Ratio [-]	FPI	thk_{fin} [mm]	Banks	Tubes per Bank	Tube Mass [kg]	Fin Mass [kg]
Baseline	7	3.63	1.79	9.621	0.1	15	15	4.68	2.8

The optimization was conducted using water as the heat transfer fluid with an inlet temperature of 50°C. The solver predicted similar relative heat load increase at both conditions. Thus, it is sufficient to evaluate new designs using only one design condition. The PCM phase-change temperature for all designs was 58°C. Each tube was divided into 10 segments. Table 5 shows the optimization problem definition.

Table 5: Optimization study problem definition

Objectives	Minimize cost (material mass) Maximize heat load
Constraints	Coil Height [m] ≤ Baseline Coil Width [m] ≤ Baseline Coil Length [m] = Baseline PCM Volume [m³] > Baseline Pressure Drop [kPa] < Baseline+50% Heat Load [kW] > Baseline
Variables	Outer Diameter [mm] Transverse Tube Pitch Ratio [-] Longitudinal Tube Pitch Ratio [-] Fin Density [FPI] Fin Thickness [mm]
Starting Population	200
Generations	2000

The objective of the study was to minimize cost and maximize heat load. Cost is defined using a function that weighs the material mass of the heat exchanger by the cost of the material. Copper is weighted higher than aluminum in this case. The variables in the study were outer tube diameter, vertical tube pitch ratio, horizontal tube pitch ratio, fin pitch, fin thickness, and tube length. The total PCM mass in the battery was constrained to be greater than or equal to the baseline value to ensure the resulting design can provide the same thermal storage potential. The heat exchanger designs were constrained to be equal to or less than the dimensions of the baseline to stay within the same battery envelope. The fluid pressure drop was constrained to be less than the baseline pressure drop +50%, to open the design space to heat exchangers with additional tube length and smaller tubes. Tube wall thickness was assumed to be an equal ratio of the tube thickness to tube diameter of the baseline design, 7-mm outer diameter to 1-mm tube thickness. All designs were assumed to use copper tubing and aluminum fins.

Figure 7 shows the results of the optimization study, showing relative cost and relative heat load against the baseline for heat exchanger designs that met all problem constraints and performed better than the baseline. The designs are colored by the fin density and sized by the total number of tubes.

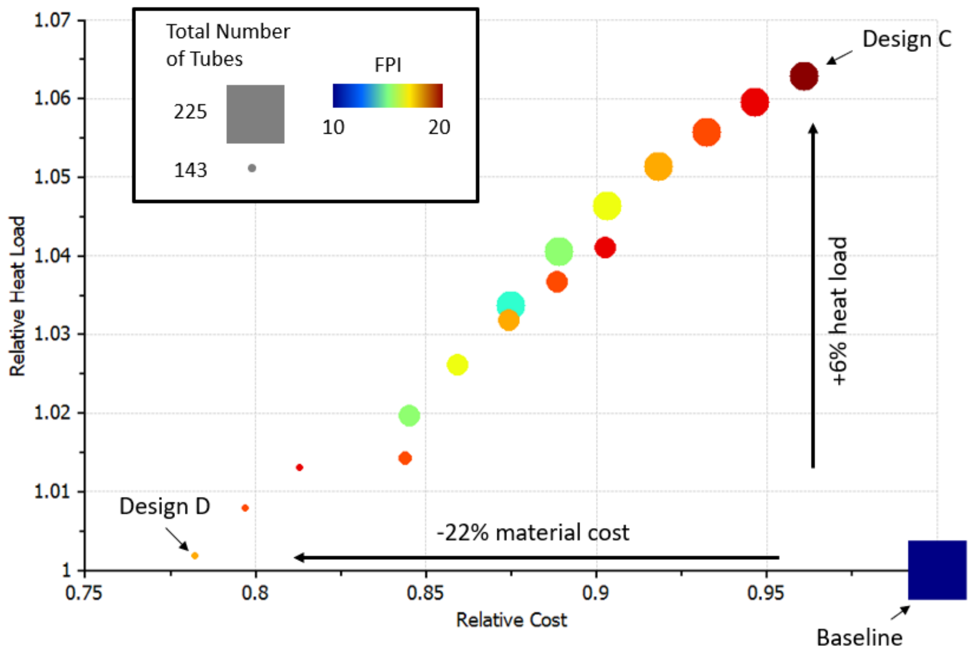

Figure 7: Optimization study results

Two heat exchanger designs were selected to show the range of potential designs that meet the problem constraints. Design C was selected as the highest heat load design that met the optimization problem constraints. Design D was selected to show potential material cost savings while meeting the same heat load. Table 6 shows the heat exchanger geometry of the selected HX designs. Table 7 shows the performance details of the selected designs against the baseline.

Table 6: HX design geometry comparison

	D_o [mm]	P_t Ratio [-]	P_l Ratio [-]	FPI	thk_{fin} [mm]	Banks	Tubes per Bank
Baseline	7	3.63	1.79	9.621	0.1	15	15
Design C	7	3.4	2.06	20	0.1	12	15
Design D	7	3.89	2.24	17	0.1	11	13

Table 7: HX design performance comparison

	Baseline	Design C	% Change	Design D	% Change
Q [kW]	35.1	37.3	6%	35.2	0%
DP [kPa]	3.608	5.33	48%	5.38	49%
Cost	14.1	13.5	-4%	11	-22%
Tube Mass [kg]	4.68	3.74	-20%	2.97	-37%
Fin Mass [kg]	2.8	5.11	83%	4.4	57%
V_{coil} [m^3]	0.0313	0.0271	-13%	0.0267	-15%
V_{PCM} [m^3]	0.0265	0.0264	0%	0.0273	3%
UA [W/K]	2227	2801	26%	2238	0%

The optimization converged on heat exchangers with the same outer tube diameter of 7 mm. The objective to minimize cost led to designs with fewer tubes and additional fin density. Both selected designs had fin density that were more than 50% denser than the baseline. This additional fin density makes up for the loss of heat exchanger area in the tubes. The aluminum fin material cost is lower than the copper tube cost, leading the solver to prioritize fin density over tubes when adding heat exchanger area.

4. DISCUSSION

4.1 Limitations of the Model / Potential Future Work

The primary advantage of using this simulation model is the rapid evaluation of many heat exchanger designs. There are a few limitations to the modeling tool:

- The model provides consistent heat exchanger performance trends but not necessarily precise absolute values.
- The modeling tool can only model the battery discharging process. For the charging process, additional test data would need to be produced and used to develop a new metamodel for thermal resistance.
- The total discharge duration is not modeled and estimated. Only the performance at a fixed inlet condition in the middle of PCM phase change is reported.
- The modeling tool has a fixed assumption for tube circuitry. Each tube bank in the vertical direction its own fluid circuit. Adding additional circuits could mitigate the effect of fluid pressure drop, and a wider range of heat exchanger designs could be evaluated.

One major challenge is the reliance of the heat exchanger solver on outputs from the transient CFD model. The transient CFD model must be used to generate the PCM thermal resistance metamodel for the solver. The metamodel is generated manually using a specific MATLAB toolbox. The metamodel is developed and verified only for a specific phase change material and tube and fin materials. In a more comprehensive version of this tool this metamodel process would be automated at runtime, either by inputting data from the transient model, or by fully running the CFD model. The challenge is how best to couple the quasi-steady state model with the CFD model.

4.1.1 Performance Degradation (Discharge Slope)

One limitation of this modeling tool is that the total discharge duration is not predicted. Heat exchanger designs are compared on heat capacity at an averaged point, and the solidification time is not determined by the model. A higher heat transfer rate will result in a faster PCM temperature drop. This could potentially mean a design with a high heat capacity could result in a heat transfer energy reduction. The transient model uses CFD simulations to determine PCM liquid fraction and temperature over time. The quasi steady-state model presented needs a means of predicting the total discharge duration. To account for this, metamodels were developed for the PCM characteristics at a range of liquid fractions. These points are then evaluated using the heat exchanger solver. A thermal resistance polynomial equation is then developed based on the results. Figure 8 shows an example of the liquid fraction data and interpolated function. An integral of this linear function is calculated using a simple trapezoid method. This new parameter, tau, can be used to evaluate relative duration of phase change between designs.

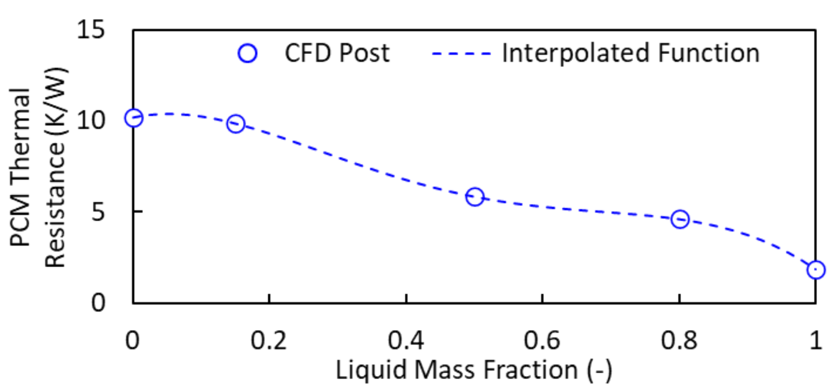

Figure 8: PCM Thermal Resistance Interpolation for Discharge Slope

5. CONCLUSIONS

A steady-state HX optimization tool for evaluating thermal battery heat exchangers at low computational cost was developed. This tool was developed to explore novel designs and aid in design selection through comparison of relative performance. The assumption for PCM thermal resistance was verified against a more detailed CFD model. The heat exchanger model was validated for quasi steady-state conditions from test data. An optimization study was conducted, yielding HX designs with potentially 6% higher heat load or at least 22% material cost reduction.

NOMENCLATURE

Parameters

D_o	Tube outer diameter	Q	Heat capacity
PtR	Transverse tube pitch ratio	thk_{fin}	Fin thickness
PlR	Longitudinal tube pitch ratio	V_{coil}	Coil envelope
FPI	Fins per inch	V_{PCM}	Volume of PCM
F_p	Fin pitch	UA	HX thermal capacitance
P_l	Longitudinal tube pitch	RPCM	Thermal resistance of PCM
P_t	Transverse tube pitch		

Abbreviations

CFD	Computational Fluid Dynamics
DP	Differential Pressure
HSLU	Hochschule Luzern (Lucerne University of Applied Sciences and Arts)
HTC	Heat Transfer Coefficient
HX	Heat Exchanger
MOGA	Multi-Objective Genetic Algorithm
PCM	Phase Change Material

REFERENCES

Blasius, P. R. (1913). Das Aehnlichkeitsgesetz bei Reibungsvorgangen in Flüssigkeiten. *Forschungsheft 131*, 1-41.

DACE – A MATLAB Kriging Toolbox, Version 2.0. (2002). Department of Informatics and Mathematical Modelling (IMM), Technical University of Denmark.

Gnielinski, V. (1976). New equations for heat and mass transfer in turbulent pipe and channel flows. *Int. Chem. Eng. 16*, 359–368.

Idel'chik, I. E. (1960). *Handbook of Hydraulic Resistance.* Moscow, Russia: Research Institute for Gas Purification.

MATLAB 9.5 and Global Optimization Toolbox 4.0. (2018). Natick, Massachusetts, United States: The MathWorks, Inc.

Neumann, H., Palomba, V., Frazzica, A., Seiler, D., Wittstadt, U., Gschwander, S., & Restuccia, G. (2017). A simplified approach for modelling latent heat storages: application and validation on two different fin-and-tubes heat exchangers. *Appl. Therm. Eng. 125*, 41-52.

Ould Didi, M. B., Kattan, N., & Thome, J. R. (2002). Prediction of two-phase pressure gradients of refrigerants in horizontal tubes. *International Journal of Refrigeration 25*, 935-947.

Shah, M. (1982). Chart Correlation for Saturated Boiling Heat Transfer: Equations and Further Study. *ASHRAE Transactions 88 (1)*, 185-196.

Waser, R., Maranda, S., & Stamatious, A. (2018). Modeling of solidification including supercooling effects in a fin-tube heat exchanger based latent heat storage. *Solar Energy*.

ACKNOWLEDGEMENT

Thank you to the International Copper Association (ICA) for helping to fund this effort. Thank you to HSLU and Remo Waser for their support of this project. Thank you to Sunamp and Dr. Maurizio Zaglio for funding and supporting this project.